Available online at www.sciencedirect.com
ScienceDirect
Geochimica et Cosmochimica Acta 71 (2007) 2264–2284
Geochimica et Cosmochimica Acta
www.elsevier.com/locate/gca

The reaction kinetics of alanine and glycine under hydrothermal conditions

Jenny S. Cox *, Terry M. Seward

Institut für Mineralogie und Petrographie, ETH-Zürich, CH-8092 Zürich, Switzerland

Received 31 March 2006; accepted in revised form 15 January 2007; available online 30 January 2007

Abstract

Experimental data on the hydrothermal reaction kinetics of α-alanine, glycine, and β-alanine were acquired using a custom-built spectrophotometric reaction cell which permits *in situ* observation under hydrothermal conditions. Quantitative kinetic information, including rate constants, concentration versus time profiles, and calculations of the individual component spectra, was obtained from the data using a self-modeling chemometric approach based on factor analysis which treats the rate expressions simultaneously as a system of differential algebraic equations (DAE) of index 1. Experimental data collected at 120–165 °C and 20 bar indicates that aqueous α-alanine, glycine and β-alanine will preferentially undergo dimerization and subsequent cyclization when heated in an inert reactor. The results presented here lend further support to the roles of temperature, exposed reactive surfaces, and matrix additives in the reaction kinetics of the structurally simple amino acids examined in this study.

1. INTRODUCTION

The discovery of the abiotic synthesis of amino acids in 1953 (Miller, 1953; Miller, 1955; Miller and Urey, 1959) and the existence of deep-sea hydrothermal vents in 1977 (Corliss et al., 1979) moved amino acids and their hydrothermal behavior to the forefront of the discussion on the relative feasibility of various geochemical environments for the origin of life. Geologically relevant scenarios that could give rise to the conditions necessary to produce and maintain reasonable concentrations of amino acids, in addition to sustaining more complex arrangements and ultimately life itself, have been a matter of some debate for decades.

Understanding and quantifying the stability of amino acids under hydrothermal conditions is of fundamental importance to these questions, but has remained elusive due to an overall lack of experimental data. The difficulties of experimentation under hydrothermal conditions and the wide variety of experimental methods and materials employed in existing studies, coupled with the apparent sensitivity of many amino acid systems to the experimental environment, has kept the rate of progress slow and led to confusion over inconsistent results.

The amino acids α-alanine and glycine are of particular interest to the discussion of hydrothermal stability because they are the simplest and smallest amino acids, as well as being among the most common and pervasive in submarine hydrothermal environments (Kohara et al., 1997; Horiuchi et al., 2004). Although previous studies have been carried out on the hydrothermal behavior of α-alanine, prior work has generally either observed or simply assumed that the preferred reaction pathway of α-alanine is decarboxylation. In most studies where decarboxylation was established as the preferred pathway, other possible pathways and products were not examined or conclusively eliminated. An overview of published experimental studies is presented in Table 1, with a focus on the details of the experimental conditions.

* Corresponding author. Present address: Department of Chemistry and Biochemistry, Arizona State University, Tempe, AZ 85287-1604, USA.
E-mail address: JCox@asu.edu (J.S. Cox).

0016-7037/$ - see front matter © 2007 Elsevier Ltd. All rights reserved.
doi:10.1016/j.gca.2007.01.020

Table 1
Detailed overview of the experimental conditions and observations of studies presenting *quantitative* kinetic information on the aqueous stability of the α-alanine and glycine systems. See also Figs. 11 and 12

Reference	Temperature Range (°C)	Pressure Range (bar)	pH	Vessel Material	Degass	Additives	Analysis Method	Observations
Overview of studies presenting quantitative kinetic information on the aqueous stability of the α-alanine system								
Abelson (1956)	Up to 450	P_{sat}	?	glass?	?	?	?	Graph of alanine breakdown presented, but no experimental details or data points are stated explicitly in the publication.
Andersson and Holm (2000)	200	50	6	teflon autoclave, stainless steel tubes	y, Ar	asp, leu, ser, KCl	sample filtered & frozen, HPLC-OPA	Alanine disappearance was modeled using first-order kinetics. Alanine possible breakdown product of other amino acids present.
Bada et al. (1995)	240	P_{sat}	7	glass tubes	y, vacuum	phosphate buffer, gly, leu, ethyl-amine	HPLC-OPA	Alanine was unstable.
Conway and Libby (1958)	25–153	P_{sat}	nat.	glass vessels	y, $+CO_2$ added	radio-labelled CO_2	detection of radiolabelled CO_2 exchanged	Alanine disappearance modeled by first-order decarboxylation.
Li et al. (2002)	280–330	275	1–9	Grade 2 Ti reactor, flow-through, sapphire windows	y, Ar	none	*in situ* observation of CO_2 production in flow-through mode by IR	Alanine breakdown modeled by first-order decarboxylation.
Li and Brill (2003a)	310–330	275	nat.	Grade 2 Ti reactor, flow-through, sapphire windows	?	none	*in situ* observation of CO_2 production in flow-through mode by IR	Alanine breakdown modeled by first-order or pseudo-first order decarboxylation.
Qian et al. (1993)	120–220	P_{sat}	nat.	glass syringes	y, N_2	none	HPLC-OPA	'No breakdown observed.' 89.2% still present at 120 °C, 504 h; 99.3% still present at 160 °C, 148 h; 93.5% still present at 220 °C, 24 h.
Qian et al. (1993)	120–220	268	nat.	glass syringes	y, N_2	none	HPLC-OPA	Alanine disappearance modeled by first-order decarboxylation.
Sato et al. (2004)	200–340	200	nat.	stainless steel 316 tube reactor, flow-through	y, ultrasonic	none	HPLC-postcolumn fluorescence; organic acid analyzer; ion chromatography	Simultaneous decarboxylation and deamination observed, primary and secondary product formation.
Snider and Wolfenden (2000)	200	P_{sat}	6.8	quartz tubes	y, vacuum	phosphate buffer	^{1}H-NMR with pyrazine standard	Alanine disappearance modeled by first-order decarboxylation.
Vallentyne (1964)	243	P_{sat}	nat.	Pyrex tubes	y, vacuum	none	TLC/ninhydrin stain	First-order decarboxylation observed, only ethylamine detected. Approx. 3% of ala remaining after 20 d at 230 °C.
JR White, as cited in Bernhardt et al. (1984)	253	260	?	?	?	buffer?	?	Dialanine was observed to undergo rapid hydrolysis.

(*continued on next page*)

Table 1 (*continued*)

Reference	Temperature Range (°C)	Pressure Range (bar)	pH	Vessel Material	Degass	Additives	Analysis Method	Observations
Kawamura et al. (2005)	275	100–150	nat.	silica fiber optic tubing, flow-through microreactor	?	none	HPLC/HPLC-chiral/ MALDI-MASS	Observed elongation of alanine oligomers. Back reactions (hydrolysis) consistent with pseudo-first-order processes. 'Since the decarboxylation of amino acids is slower than the formation of DKP, the decarboxylation can be ignored in these systems.'
Kawamura and Yukioka (2001)	275	100	7.0	teflon autoclave, stainless steel tubes	?	NaCl, $MgCl_2$, HCl, NaOH	HPLC with chiral separation	L-ala-L-alanine underwent cyclization to alanine anhydride (DKP).
Overview of studies presenting quantitative kinetic information on the aqueous stability of the glycine system								
Qian et al. (1993)	120–220	P_{sat}	nat.	glass syringes	y, N_2	none	HPLC-OPA	Only minor gly breakdown observed. 86.4% still present at 120 °C, 504 h; 100% still present at 160 °C, 148 h; 80.1% still present at 220 °C, 24 h.
Qian et al. (1993)	120–220	268	nat.	glass syringes	y, N_2	none	HPLC-OPA	Glycine disappearance modeled by first-order decarboxylation. Gly-gly decomposition rates several orders of magnitude faster than gly.
Sato et al. (2002)	260–340	300						Glycine both decarboxylated and deaminated, with an overall first-order trend. Reference in Japanese.
Sato et al. (2004)	200–340	200	nat.	stainless steel 316 tube reactor, flow-through	y, ultrasonic	none	HPLC-postcolumn fluorescence; organic acid analyzer; ion chromatography	Simultaneous decarboxylation and deamination observed, primary and secondary product formation.
Snider and Wolfenden (2000)	170–260	P_{sat}	6.8	quartz tubes	y, vacuum	phosphate buffer	^{1}H-NMR with pyrazine standard.	Glycine disappearance modeled by first-order decarboxylation.
Cronin et al. (1971)	95	?	5.6	?	?	0.04 M Zn(II)	Beckman Analyzer with ninhydrin detection	Observations of Zn catalysis of cyclic peptide formation as well as hydrolysis. Rates in absence of Zn were 'very slow' and not determined.
Fujii et al. (2002)	70	open air	8.1	glass	no	0.075 M HEPES	HPLC	Pseudo first-order rate constant determined for hydrolysis of gly-gly.
Haramaki and Nakashima (2001)	119–167	?	?	?	?	?	ATR-IR spectroscopy and HPLC	Unpublished data in book chapter. Thermal decomposition of gly-gly.
Li and Brill (2003b)	310–330	275	nat.	Grade 2 Ti reactor, flow-through, sapphire windows	?	none	*in situ* observation of CO_2 production in flow-through mode by IR	Gly-gly disappearance modeled by first-order or pseudo-first order decarboxylation.
Radzicka and Wolfenden (1996)	25–181	P_{sat}	6.8	quartz tube	y, vacuum	0.1 M phosphate or acetate buffer; KCl to I = 2.0	^{1}H-NMR	Gly-gly hydrolysis observed to follow first-order kinetics, and cyclization produced DKP product. Equilibrium constant measured for gly-gly/DKP interconversion.

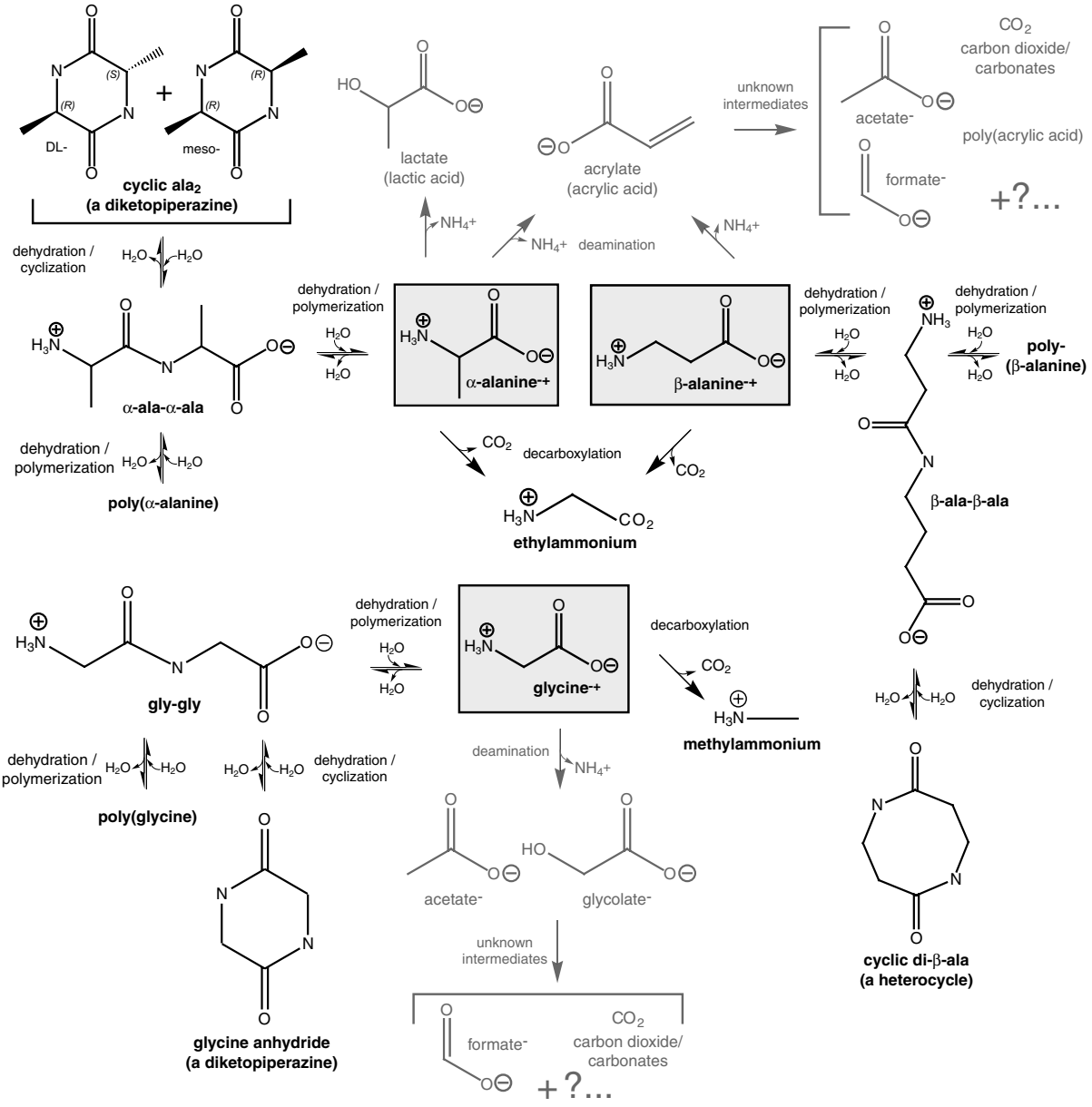

Fig. 1. Theoretically feasible reaction pathways of α-alanine, β-alanine, and glycine and their products under degassed aqueous conditions. Pathways discussed in detail are indicated in black.

Several notable exceptions to the general observations of breakdown of α-alanine have recently been published. For example, Kawamura and Yukioka (2001) observed α-alanine to preferentially dimerize and then rapidly cyclize at 275 °C in a flow-through reactor, as part of a quantitative study which originally intended to determine thermal racemization kinetics. Ogata et al. (2000), and later Yokoyama et al. (2003) using a similar experimental setup, qualitatively observed both alanine and glycine dimerization and oligomerization up to tetrapeptides at 250 °C in a flow-through reactor designed to simulate a hydrothermal vent. Alanine and glycine were also observed to co-polymerize in solution. Sato et al. (2004) despite observing mostly decarboxylation and deamination, provide an unusually thorough attempt at product characterization.

In the case of glycine, several other studies have reliably observed the production of oligopeptides (up to 13 units) and cyclic dimers (diketopiperazines) under hydrothermal conditions. This is particularly true with glycine reactions in 'simulated hydrothermal vent' type reactors (Imai et al., 1999a,b; Ogata et al., 2000; Alargov et al., 2001; Alargov et al., 2002; Tsukahara et al., 2002; Islam et al., 2003; Yokoyama et al., 2003; Mitsuzawa and Yukawa, 2004; Faisal et al., 2005; Goto et al., 2005; Kawamura et al., 2005; Shiota and Nakashima, 2005). In the majority of cases,

due to the number of products produced and the overall complexity of the system, the authors were unable to determine quantitative kinetics and rate constants but provided concentration versus time data.

The study presented here focuses on the acquisition of basic experimental kinetic data on the hydrothermal behavior of the amino acids α-alanine, glycine and β-alanine. Quantitative experimental data on these amino acids were determined, with an emphasis on acquiring the kinetic data *in situ* and using an inert reaction vessel. These data are among the first directly observed, real-time observations of amino acids reacting under hydrothermal conditions (Cox and Seward, 2007).

A diagram of the theoretically feasible breakdown pathways of α-alanine, glycine and β-alanine is presented in Fig. 1, along with the pathways of the major primary and secondary reaction products. This diagram is intended as a general overview presenting anticipated possibilities, since primary pathways are observed to vary depending upon experimental conditions. Pathways specifically observed or discussed in this study are indicated in bold.

2. EXPERIMENTAL PROCEDURE

2.1. Materials and methods

The high-temperature spectrophotometric cell built specifically for this project permitted in situ observation of amino acid solutions under the chosen conditions of temperature and pressure. The cell design and its flow-through setup were previously described in Cox and Seward (2007). The spectrophotometric reactor cell was constructed such that the amino acid solutions were only in contact with the pure gold liner and the high purity UV optical silica windows. Gold-lined pressure tubing was used to interface the cell to the inert polyetheretherketone polymer (PEEK) high pressure flow-through lines, to ensure that the entire flowpath seen by the solutions was as inert as possible. The ultraviolet spectra themselves arise from electronic transitions in the molecules and are characteristic of each component present in the solution. The amino acid zwitterions and their breakdown products (protonated or unprotonated) have unique electronic spectra which are intimately related to the structure of the compound. Measured absorbance (A) is directly proportional to concentration (c) as per the Beer–Lambert Law, $A = \varepsilon bc$, where ε is the molar absorptivity coefficient, which is specific to a given molecule, and b is the path length of the light through the solution.

Our hypothesis at the time of construction, later confirmed experimentally, was that the composition of the reaction vessel materials can fundamentally affect the behavior of the solutions being observed. Our results indicate that the kinetics of aqueous amino acid solutions can be significantly altered by the presence of traditional metal alloys and other catalytic surfaces, as discussed in detail by Cox and Seward (2007).

All solutions (from 5.15×10^{-4} mol dm^{-3} to 2.88×10^{-3} mol dm^{-3} ± 0.1–0.2%) used in this study were freshly prepared from 18 mΩ 0.2 μm nylon-membrane filtered high purity water, without the addition of buffers or other components. The pH in these dilute, degassed solutions was defined by the water and amino acid activity and was close to neutral; a more detailed discussion of speciation and pH with temperature is presented in Section 3.1 below. The glycine, L-α-alanine and β-alanine used in this study were either Fluka Microselect Grade or SigmaUltra Grade (Sigma–Aldrich Chemical Group, Germany), with purities of 99.0–99.5% depending on the compound. After preparation, solutions were transferred into a dry, sterile flask, and thoroughly degassed using a combination of He (Pangas, 99.9995%, filtered) sparging and an online vacuum degassing unit. The degassed solution was then pumped into the flow-through line connected to the combination optical cell/reaction vessel installed in the sample compartment of the spectrophotometer (Varian Cary 4E with WinUV 2.0 software). The cell was heated *in situ* while in flow-through mode until equilibration was reached at the chosen temperature and pressure, and the reaction was allowed to proceed by stopping the flow of solution to enable the observation of one batch. UV absorption scans of 0.2 nm resolution were taken at regular time intervals (2–10 min) and under appropriate spectrophotometric instrumental conditions in order to obtain kinetic information. When data collection and observation were completed, the system was again set to flow-through mode and ultrapure water was circulated until the cell was completely flushed. Once thorough flushing had been assured, a set of background blank spectra (windows + H_2O) was taken under the same conditions and instrumental parameters as the experiment. Raw spectral data were later corrected by subtraction of blank spectra, as well as mathematically corrected to take into account the changes in solution density (i.e. water) with temperature and pressure. The number of absorbing species, the chemical model, and individual component spectra were determined using a mathematical factor analysis based approach, with the kinetics of the system being inherently determined as part of the mathematical analysis procedure. Samples were also taken for ion chromatographic analyses to confirm the identities of the products, but due to the low concentrations involved in the experiments, this approach was not always conclusive.

2.2. Mathematical analysis

This study employed a chemometric approach based on factor analysis (similar to principle component analysis, PCA) in order to obtain kinetic information from the acquired data. Mathematical factor analysis can be meaningfully applied to this study because the data represent the change in time of a chemical system, as determined by the kinetic interrelation between the chemical species, and the UV spectra taken at each time interval thus have a mathematical relationship with each other.

An overview of the mathematical analysis procedure, together with the key equations, is presented in flowchart

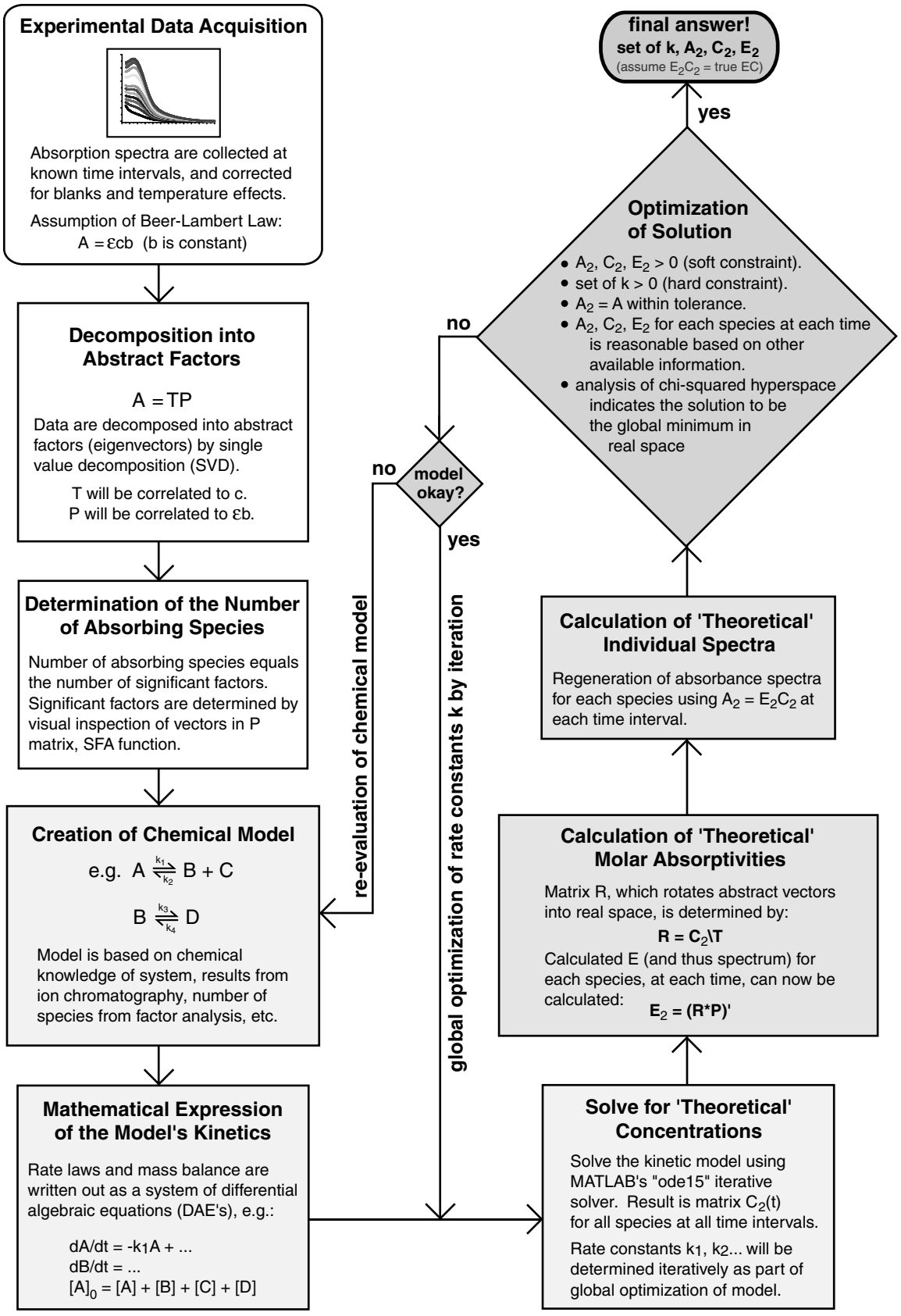

Fig. 2. Flowchart representing the mathematical analysis of spectrophotometric data in order to obtain kinetic information.

form in Fig. 2. Unlike traditional deconvolution, this method regenerates the spectra from a globally optimized solution based on the data's principle factors and a chemical model; this type of 'self-modeling' approach does not require any *a priori* information about the system. This approach is more robust and removes the uncertainties associated with 'curve fitting' and other deconvolution procedures, from which it should be distinguished, where the resulting assignment of the individual species' spectra are frequently arbitrary. The reader is referred to Malinowski (1991) for a detailed overview and discussion of this method as well as principle component analysis and factor analysis in general, beyond what is presented in this study, which follows the exact methodology of the related study by Cox and Seward (2007). The mathematical analysis and calculations were performed on the Matlab 6 R12/R13 program platform (Mathworks, Inc., 2000), using functions and scripts specifically developed for this study.

3. RESULTS

3.1. The α-alanine system

3.1.1. Experimental data

Ultraviolet spectrophotometric data of the real-time, *in situ* thermal evolution of aqueous α-alanine solutions with time were collected at 5 min intervals over periods of several hours. This was repeated at various temperatures between 120 and 183 °C. It was not possible to quantita-

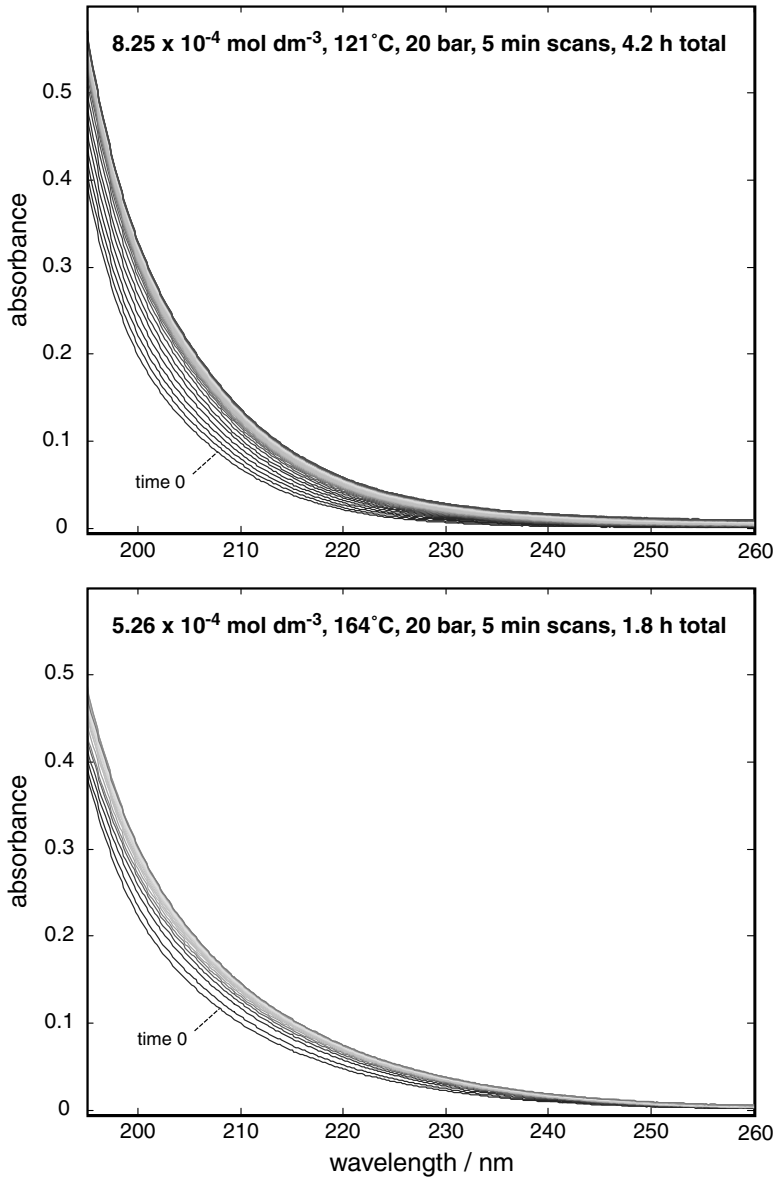

Fig. 3. Two examples of UV absorption data sets collected in situ of the thermal evolution of α-alanine solutions in an 'inert' reactor: 121 °C (top) and 164 °C (bottom).

tively solve data at the higher end of the temperature range because only slight changes with time were recorded, which led to the mathematical system becoming ill-defined. Two examples of spectrophotometric data sets are presented in Fig. 3. All of the sets exhibit the same general behavior of a slow increase in absorption over all wavelengths with time, with a significant increase occurring in the 190–240 nm region. This was contrary to the initial expectations of the behavior of this system, since α-alanine has been generally considered to decarboxylate, which produces smaller molecules with lower absorbances in the observed range. Breakdown, in general, is expected to produce smaller and less electronically conjugated molecules, and to be observed as a decreasing absorption with time which approaches zero baseline. In this study the opposite trend, increasing absorption, was observed to be true. Additionally, three absorbing species were determined by factor analysis to be present, indicating that two separate products were produced in statistically significant quantities.

Secondary analyses by ion chromatographic amino acid analysis (High Pressure Anion Exchange Chromatography with Pulsed Amperometric Detection (HPAEC-PAD) using a Dionex instrument and AminoPAC column) were not conclusive in this case and detected only the presence of the α-alanine monomer. Several obstacles existed to the analyses, in particular the overlapping elution times of α-alanine, dialanine, and cyclic dialanine (a diketopiperazine). This not only made resolution difficult, but in the case where one compound is present in much larger quantities than the others (as is the case here for α-alanine), the larger peak signal swamps the other signals entirely. Additionally, this analytical method has a low sensitivity to cyclic dialanine because it does not have amine or carboxylic functional groups. It was not possible to build up enough products, even in flow-through mode, to be able to fully overcome these issues.

3.1.2. *Mathematical factor analysis*

Mathematical factor analysis was employed to extract quantitative kinetic information from the UV absorption scans. Factor analysis/singular value decomposition indicated the definite presence of three absorbing factors in all data sets for the α-alanine system. The first factor could be clearly attributed to α-alanine, which is the dominant species. The remaining factors were determined through model testing and chemical reasoning.

The first step towards building relevant possible chemical models was to determine the speciation of α-alanine, given the possibility that different species might react at different rates (thus the significance of examining rate versus pH) as well as exhibit different absorption spectra. An estimation of the expected speciation of aqueous α-alanine at zero ionic strength from 25 to 200 °C was made based on isocoulombic extrapolations (Lindsay, 1980) of ionization constant data up to 50 °C (Nims and Smith, 1933; Smith et al., 1937; and Christensen et al., 1968) and more recent data up to 125 °C (Gillespie et al., 1995; Wang et al., 1996). This well-defined trend can be extrapolated with confidence to estimate the higher temperature ionization behavior of α-alanine. Based on this method, at neutral pH and 25 °C, α-alanine exists solely as the $Hala^{-+}$ zwitterion, where the carboxylic group is deprotonated and the amino group is protonated. With increasing temperature, the $Hala^{-+}$ zwitterion region of α-alanine shifts mostly in tandem with pK_w, and up to 185 °C the fraction of $Hala^{-+}$ present at neutral pH is estimated to be consistently greater than 97.5%. Solutions of dilute α-alanine, unadjusted with respect to pH, are therefore expected to contain α-alanine in almost entirely the $Hala^{-+}$ zwitterionic form up to 185 °C.

Relevant chemical models which included three absorbing species and were based on polymerization, decomposition, or a combination of the two, were tested on each data set such that the correct model could be determined by both 'goodness of fit' criteria and by a process of elimination. The models tested, the chemical systems they represent, and their resulting kinetic information are presented in Table 2. Every chemically reasonable model was tested against each data set.

Of all 14 chemically reasonable models tested, only **Model 1** was capable of providing a good fit to the data (**System of Equations 1**). This model also fitted every data set, implying that the nature of the kinetic system is constant across temperature. **Model 1** is based on a "2 alanine → primary products → secondary products" type system. **Model 1** (**System of Equations 1**)

$$\begin{aligned} d[ala]/dt &= -2k_1[ala]^2 \\ d[ala_2]/dt &= +k_1[ala]^2 - k_2[ala_2] \\ d[\text{cyclic ala}_2]/dt &= +k_2[ala_2] \\ [ala] &= [ala]_0 - 2[ala_2] - 2[\text{cyclic ala}_2] \end{aligned}$$

The other tested models were all found to be insufficient. Models having reversible reactions were found to have optimum convergence at the limit where they reduced to the same behavior as **Model 1**; this is likely due to the timescale of the experiments presented here, as one would expect reversibility and attainment of equilibrium over longer timescales. **Models 8–14** either did not converge, or converged in the limit where they reduced to the same behavior as **Model 1**. **Models 2 and 3** were tested to eliminate the possibility of other reaction orders. These models included a scenario in which the "2 alanine → dialanine" reaction is first order or 4/3 order with respect to alanine according to Permyakov et al. (2002), who recently showed evidence suggesting that the dimerization of amino acids may proceed by non-integral orders and that this effect is pair-specific. The second reaction is generally held to progress by first order or pseudo-first order (i.e. solvent assisted) kinetics (e.g. Capasso et al., 1998). **Models 2 and 3** fitted poorly compared to **Model 1** in which the same reaction is second order with respect to α-alanine.

Model 1 was therefore the chosen model for all α-alanine data because it met the necessary criteria on several levels. It provides an excellent fit with low residuals, molar absorptivities and spectra which are consistent with known standards, and the produced rate constants are consistent with the small amount of α-alanine literature data to date on dimerization and cyclization (Kawamura and Yukioka, 2001; Cox and Seward, 2007). Lastly, in addition to being

Table 2
Models tested for the 'inert reactor' aqueous α-alanine acid system, and the rate constants and kinetic information derived from **Model 1** for α-alanine

Model	Model description (speciation not indicated)			Reaction order	Result	Acceptable
1 n = 3	2 ala	—k_1→	$ala_2 + H_2O$	k_1—second order	**excellent fit, low residuals**	**yes**
	ala_2	—k_2→	cyclic $ala_2 + H_2O$	k_2—first order		
2 $n = 3$	2 ala	—k_1→	$ala_2 + H_2O$	k_1—first order	poor fit	no
	ala_2	—k_2→	cyclic $ala_2 + H_2O$	k_2—first order		
3 $n = 3$	2 ala	—k_1→	$ala_2 + H_2O$	k_1—4/3 order	poor fit	no
	ala_2	—k_2→	cyclic $ala_2 + H_2O$	k_2—first order		
4 $n = 3$	2 ala	—k_1→	$ala_2 + H_2O$	k_1—second order	converges at limit where	no
	ala_2	—k_2→	cyclic $ala_2 + H_2O$	k_2—first order	model 4 approaches model 1	
		←k_3—		k_3—pseudo first order		
5 $n = 3$	2 ala	—k_1→	$ala_2 + H_2O$	k_1—second order	converges at limit where	no
		←k_2—		k_2—pseudo first order	model 5 approaches model 1	
	ala_2	—k_3→	cyclic $ala_2 + H_2O$	k_3—first order		
6 $n = 3$	2 ala	—k_1→	$ala_2 + H_2O$	k_1—second order	converges at limit where	no
		←k_2—		k_2—pseudo first order	model 6 approaches model 1	
	ala_2	—k_3→	cyclic $ala_2 + H_2O$	k_3—first order		
		←k_4—		k_4—pseudo first order		
7 $n = 3$	2 ala	—k_1→	$ala_2 + H_2O$	k_1—second order	does not converge	no
	ala_2	=	cyclic $ala_2 + H_2O$	K_{eq} = equilibrium const.		
8 $n = 3$	2 ala	—k_1→	$ala_2 + H_2O$	k_1—second order	converges at limit where	no
	ala_2	—k_2→	cyclic $ala_2 + H_2O$	k_2—first order	model 8 approaches model 1	
	$ala + H_2O$	—k_3→	ethylamine + CO_2 + OH^-	k_3—pseudo first order		
9 $n = 3$	2 ala	—k_1→	$ala_2 + H_2O$	k_1—second order	converges at limit where	no
	ala_2	—k_2→	cyclic $ala_2 + H_2O$	k_2—first order	model 9 approaches model 1	
		←k_3—		k_3—pseudo first order		
	$ala + H_2O$	—k_4→	ethylamine + CO_2 + OH^-	k_4—pseudo first order		
10 $n = 3$	2 ala	—k_1→	$ala_2 + H_2O$	k_1—second order	converges at limit where	no
		←k_2—		k_2—pseudo first order	model 10 approaches model 1	
	ala_2	—k_3→	cyclic $ala_2 + H_2O$	k_3—first order		
	$ala + H_2O$	—k_4→	ethylamine + CO_2 + OH^-	k_4—pseudo first order		
11 $n = 3$	2 ala	—k_1→	$ala_2 + H_2O$	k_1—second order	converges at limit where	no
		←k_2—		k_2—pseudo first order	model 11 approaches model 1	
	ala_2	—k_3→	cyclic $ala_2 + H_2O$	k_3—first order		
		←k_4—		k_4—pseudo first order		
	$ala + H_2O$	—k_5→	ethylamine + CO_2 + OH^-	k_5—pseudo first order		
12 $n = 3$	2 ala	—k_1→	$ala_2 + H_2O$	k_1—second order	does not converge	no
	$ala + ala_2$	—k_2→	$ala_3 + H_2O$	k_2—second order		
13 $n = 3$	2 ala	—k_1→	$ala_2 + H_2O$	k_1—second order	does not converge	no
	$ala + ala_2$	—k_2→	$ala_3 + H_2O$	k_2—second order		
	$ala + H_2O$	—k_3→	ethylamine + CO_2 + OH^-	k_3—pseudo first order		
14 $n = 3$	2 ala	—k_1→	$ala_2 + H_2O$	k_1—second order	does not converge	no
		←k_2—		k_2—first order		
	$ala + H_2O$	—k_3→	acrylate + NH_4^+	k_3—pseudo first order		

Temp (°C)	No. of scans used	Factors	Model	Rate constant k_1 (mol^{-1} dm^3 s^{-1})[a]	Rate constant k_2 (s^{-1})[a]	Instrumental error	Standard deviation of model [b]
120.9 ± 0.4	51	3	1	$5.4 \times 10^{-2} \pm 0.2 \times 10^{-2}$	$4.45 \times 10^{-4} \pm 0.01 \times 10^{-4}$	2.0×10^{-4}	4.9×10^{-4}
131.6	53	3	1	$6.8 \times 10^{-2} \pm 0.2 \times 10^{-2}$	$5.60 \times 10^{-4} \pm 0.01 \times 10^{-4}$	2.0×10^{-4}	3.6×10^{-4}
145.1	46	3	1	$1.07 \times 10^{-1} \pm 0.01 \times 10^{-1}$	$1.053 \times 10^{-3} \pm 0.002 \times 10^{-3}$	2.1×10^{-4}	3.6×10^{-4}

(*continued on next page*)

Table 2 (*continued*)

Temp (°C)	No. of scans used	Factors	Model	Rate constant k_1 (mol^{-1} dm^3 s^{-1})[a]	Rate constant k_2 (s^{-1})[a]	Instrumental error	Standard deviation of model [b]
154.7	30	3	1	$3.42 \times 10^{-1} \pm 0.05 \times 10^{-1}$	$1.224 \times 10^{-3} \pm 0.008 \times 10^{-3}$	2.1×10^{-4}	6.3×10^{-5}
162.3	30	3	1	$4.79 \times 10^{-1} \pm 0.02 \times 10^{-1}$	$5.3 \times 10^{-3} \pm 0.2 \times 10^{-3}$	2.1×10^{-4}	2.0×10^{-4}
164.0	23	3	1	$8.05 \times 10^{-1} \pm 0.04 \times 10^{-1}$	$2.30 \times 10^{-3} \pm 0.06 \times 10^{-3}$	2.0×10^{-4}	2.5×10^{-4}
183.1	Spectra from each scan were too close together to solve mathematically						

[a] Error shown is derived from an estimated experimental error margin (5%). In all cases the 3σ confidence limit of the model convergence was very narrow, so the experimental error is taken to be more accurate.
[b] Estimated from the sum of squares of the residuals divided by the number of scans.

one of the most chemically reasonable models and one of the most simple, all other reasonable potential models were conclusively eliminated.

Although secondary confirmation of the identity of the products was inconclusive, certain important conclusions can still be inferred from the experimental data which are consistent with the choice of **Model 1**:

(1) The absorption envelope increases with time, which would only be possible if species of higher molar absorptivity were being produced. Given that the structure of α-alanine (Fig. 1) has only one carboxylic and one amine functional group, and no double bonds or aromatic groups, the most likely explanation for the higher molar absorptivity products is that alanine is dimerizing or polymerizing and forming species that are electronically more conjugated.
(2) The breakdown of α-alanine to any significant degree was not indicated in this study, since (a) any significant breakdown would lead to an overall decrease of absorption with time due to the production of even smaller and less conjugated molecules, and (b) flow-through sampling over several hours and subsequent ion chromatographic analyses did not indicate any significant disappearance of α-alanine.
(3) Oligomerization and cyclization are established pathways for glycine (e.g. Radzicka and Wolfenden, 1996; Imai et al., 1999a,b; Ogata et al., 2000; Faisal et al., 2005), which differs from α-alanine only by the replacement of a methyl group with hydrogen.
(4) Previous studies indicate that α-alanine can be quite stable under certain hydrothermal conditions (Qian et al., 1993), that polymerization of α-alanine is highly favored at much higher temperatures such as 275 °C (Kawamura and Yukioka, 2001), and that dimerization, cyclization and oligomerization have been previously observed for α-alanine but not quantified (Ogata et al., 2000; Yokoyama et al., 2003; Kawamura et al., 2005).

The rate constants derived from the application of **Model 1** to the experimental data are presented in Table 2 and Fig. 4. The application of weighted linear least squares regression to the data was used to obtain the Arrhenius parameters E_a and $\ln A$, where E_a is the apparent activation energy in kJ mol^{-1} and A is the pre-exponential factor in units of mol^{-1} dm^3 s^{-1} (k_1) or s^{-1} (k_2). For the k_1 data, $E_a = 114$ kJ mol^{-1} and $\ln A = 31$ were obtained ($R_2 = 0.88$), and for the k_2 data, $E_a = 74$ kJ mol^{-1} and $\ln A = 15$ were obtained ($R_2 = 0.78$). There were no literature values available for comparison, since only two previous studies have quantitatively examined dimerization or cyclization in α-alanine or glycine (Radzicka and Wolfenden, 1996; Kawamura and Yukioka, 2001) and neither of these studies had enough information to derive Arrhenius parameters. Cronin et al. (1971) present glycylglycine and glycylalanine data, but these were acquired in the presence of 0.04 M Zn (II), a catalyst. Kawamura and Yukioka (2001) did however derive an apparent activation energy for the racemization of α-alanine, which was determined to be 124 kJ mol^{-1}. This indicated that dimerization and cyclization are pathways which are very competitive with racemization since the activation energies are very similar within experimental error. This observation is further consistent with their observation that the formation of cyclic dialanine was faster than racemization.

The calculated molar absorptivity spectra for **Model 1** are presented for four data sets in Fig. 5. An example of a calculated concentration profile and calculated individual species absorbance spectra are presented for 145 °C in Fig. 6. A comparison between an experimental data set and the calculated overall absorbances, including residuals, is presented for 155 °C in Fig. 7.

3.2. The glycine and β-alanine systems

3.2.1. Experimental data

Several ultraviolet spectrophotometric kinetic data sets for glycine and β-alanine were acquired in a similar manner as for α-alanine, in order to provide a basis for comparison among these structurally similar compounds. Examples of spectrophotometric data sets for glycine and β-alanine are presented in Fig. 8. These data also exhibited increasing absorbance with time, similarly to α-alanine. This was particularly true of the β-alanine system, which exhibited the largest increase in absorbance of the three amino acids studied.

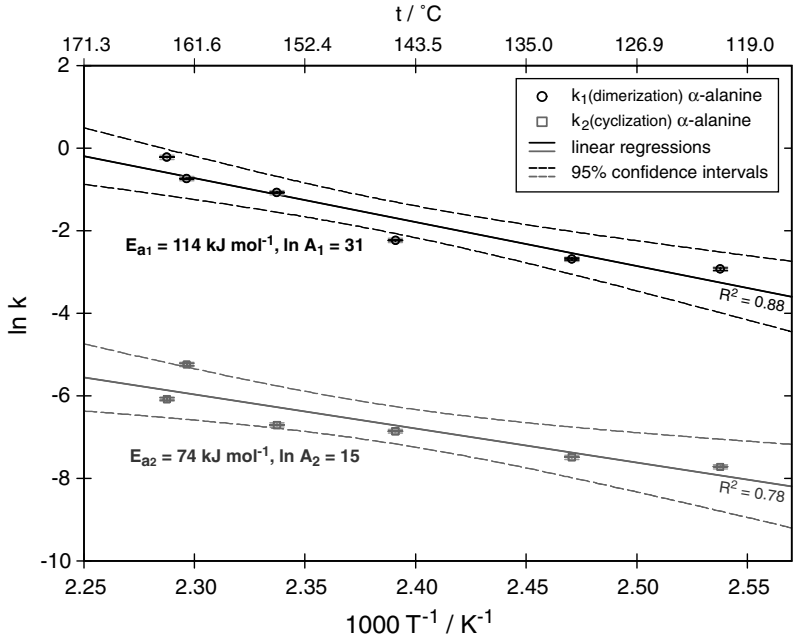

Fig. 4. Graphical representation of the rate constants, k, derived from the application of **Model 1** to the experimental data for α-alanine. Model errors and experimental errors yielded error bars no larger than the symbols; overall error is best represented by the 95% confidence interval (dotted lines). Rate constants are in units of $mol^{-1}\ dm^3\ s^{-1}$ (k_1) and s^{-1} (k_2).

3.2.2. Mathematical factor analysis

Mathematical factor analysis was applied to the data in the manner previously described for α-alanine. The presence of three absorbing factors in all data sets was also observed. Analogous models to the α-alanine system were tested, and the best fitting models were equivalent to α-alanine **Model 1**. Other models were eliminated in a similar way as for α-alanine. Quantitative kinetic information derived from the application of **Model 1** to the experimental data for glycine and β-alanine is presented in Table 3. Examples of their respective molar absorptivities and concentration profiles are presented in Fig. 9. A comparison between the experimental data set for β-alanine and its calculated overall absorbances, including residuals, is presented in Fig. 10.

4. DISCUSSION

Comparisons of the kinetic data derived in this study with the published data on α-alanine, glycine, β-alanine, and their respective oligomers, are presented as van't Hoff plots in Figs. 11 and 12.

Several previous studies have observed the polymerization of α-alanine, although only Kawamura and Yukioka (2001) were able to derive quantitative kinetic information. Their observations on the hydrothermal behavior of α-alanine in stainless steel tubing indicated that it rapidly dimerized to dialanine and then cyclized to cyclic dialanine, along with the formation of additional unidentified polymers. A rate constant for the dimerization of α-alanine at 275 °C and 200 bar was provided, however, it was not strictly considered by the authors to be a dimerization constant; as a result of the rapidity of the formation of cyclic dialanine ('alanine anhydride') from α-alanine, dialanine was an intermediate and was not directly detected. They modeled the reaction as ala + ala → alanine anhydride (k_{pip}), and since dimerization was considered to be the rate determining step, k_{pip} was 'considered to be approximately equal to' k_{dim}. The fact that their rate constant was inferred may account for the discrepancy between their value and the values presented here in this study. Conversely, their value for the cyclization of the dialanine dipeptide was determined by directly and separately measuring the reaction dialanine → alanine anhydride, and is in good agreement with the trend of the data presented here. No additional literature values for dimerization or cyclization rate constants were located for α-alanine.

Taking into consideration studies which were only qualitative, several other studies have also made observations on the polymerization of α-alanine. Clarke and Tremaine (1999) qualitatively observed that the primary hydrothermal reaction pathways of α-alanine were polymerization and decarboxylation. Li and Brill (2003a), using a grade 2 titanium reactor, observed cyclic dialanine to be stable on the time scales accessible by their experimental method, and were therefore unable to observe hydrolysis or breakdown as for cyclic diglycine. Bernhardt et al. (1984), looking specifically at degradation, estimated the half-life of dialanine as approximately 6 min, although this information was cited as having originated from a personal communication of RL White and the experimental conditions are unknown. Kawamura et al. (2005) deliberately chose to study the kinetics of larger oligomers of α-alanine (up to ala_5) precisely because of the tendency for α-alanine monomers and dimers to quickly form cyclic dialanine. They found strong evidence to support the production of larger

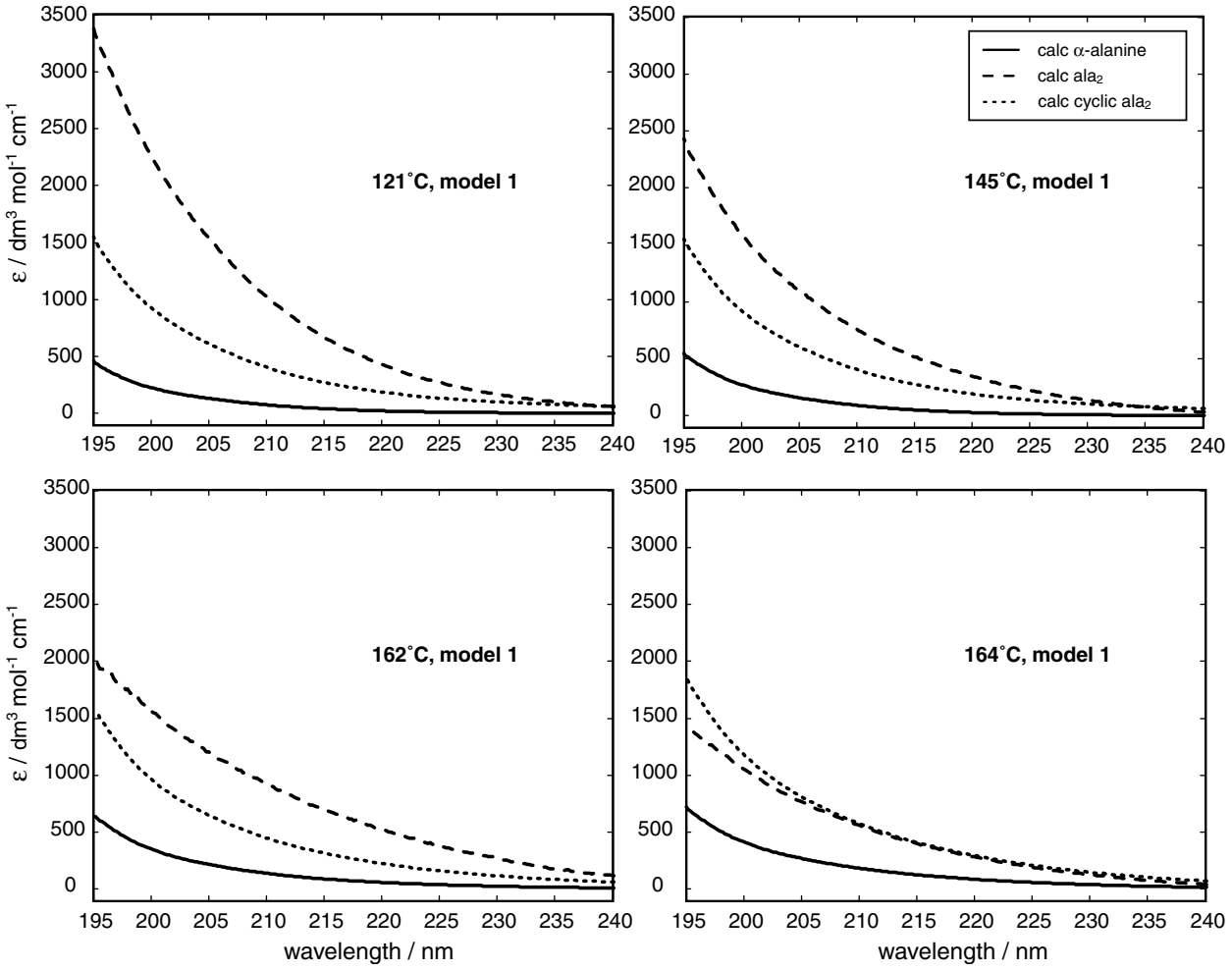

Fig. 5. Calculated molar absorptivities of α-alanine, dialanine, and cyclic dialanine at four temperatures at 20 bar. The calculated alanine spectra match those of the time zero spectra. There is an increased uncertainty at 164 °C due to the similarity of the individual molar absorptivities, causing the model to be ill-defined.

oligomers, up to ala_{13}, in the simulated hydrothermal vent reactor which was employed in their study. The process appeared to be most efficient (>10%) when starting with a tetrapeptide or larger, in the presence of an excess of monomer. Kawamura et al. (2005) also stated that decarboxylation could be ignored in their system since it was much slower than the formation of diketopiperazines. Unfortunately, no attempts at calculating rate constants for dimerization, oligomerization or cyclization were made.

The rate constants derived for dimerization in this study, as well as those of Kawamura and Yukioka (2001), were significantly higher than those for other reactions such as decarboxylation as determined by other published studies. This is consistent with the hypothesis that dimerization can be the favored pathway under certain subsets of conditions, as discussed below, as well as certain initial concentrations, given that these are second order constants. Similarly, rate constants for cyclization were higher than those for hydrolysis, supporting evidence that cyclization can also be competitive with hydrolysis and exhibit a 'protective' effect.

The question remains as to why other studies have tended to observe decomposition reactions instead of polymerization (Table 1). As previously discussed above, important uncertainties may have resulted from aspects of the experimental methods used in previous studies. Perhaps most significantly, many studies have measured the stability of alanine and glycine monomers or dimers without looking for, or being able to detect, polymeric products, according the analytical methodologies employed. Accurate determination of all major products, as well as mass balances, remains elusive in general. Also notable is the use of reactors or apparatus constructed from transition metal alloys (such as stainless steels or titanium alloys) or other materials which are known to have catalytic effects (e.g. Bell and Palmer, 1994; Bell et al., 1994). It is possible that at higher temperatures, these effects are reduced or the polymerization becomes much more favorable, which may account for why Kawamura and Yukioka (2001) were able to observe polymerization. Pressure may also play an important role in these systems; Qian et al. (1993) observed

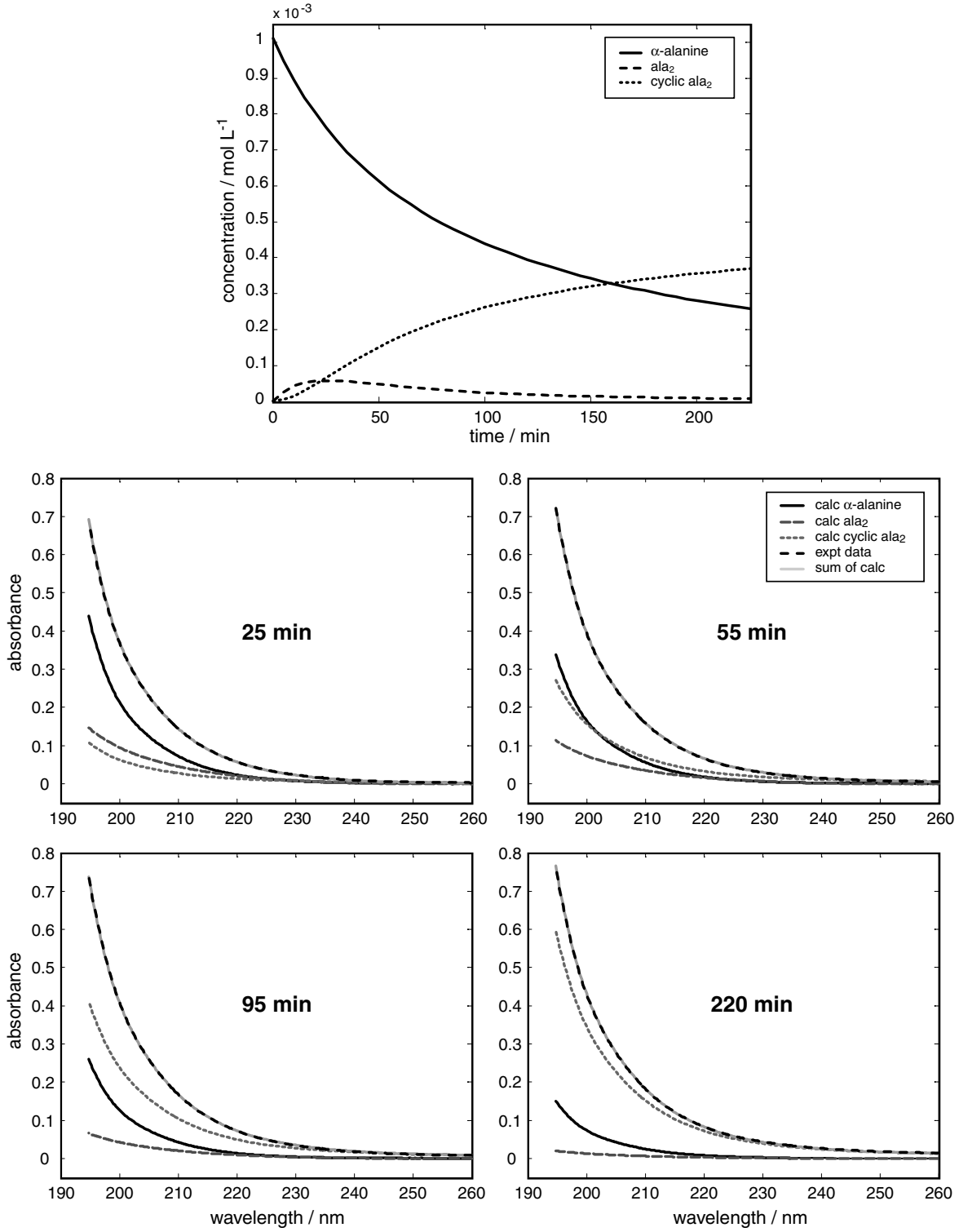

Fig. 6. Calculated concentration profiles versus time (top) and calculated individual absorption spectra at four times (bottom) for the reactions of a 1.01×10^{-3} mol dm^{-3} aqueous α-alanine solution at 145 °C and 20 bar.

that α-alanine decomposed only very negligibly in the experiments performed at saturated vapour pressure, in contrast to experiments performed at 268 bar in which there was considerable breakdown. The decomposition under 'low pressure' conditions (up to 160 °C and 504 h) was slow enough for glycine and α-alanine that it was not possible for

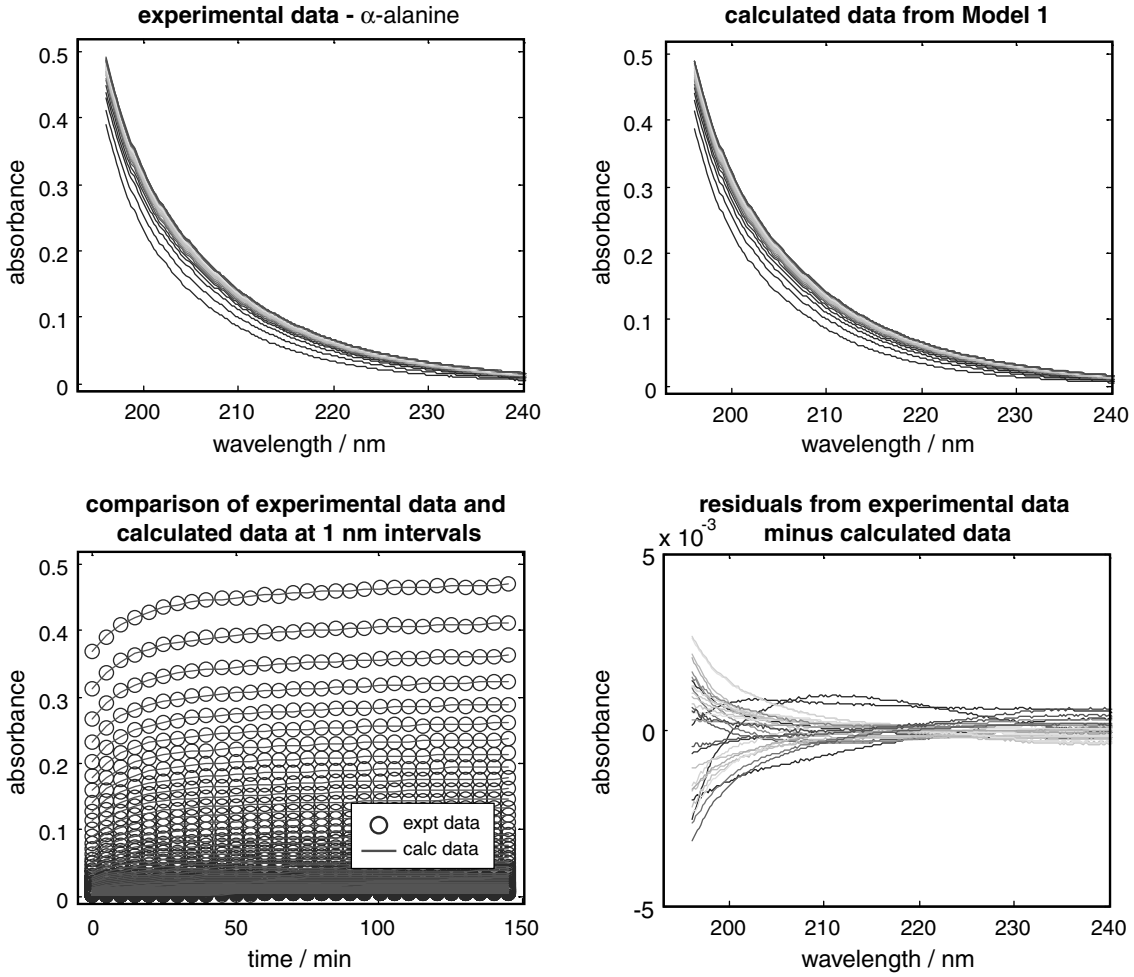

Fig. 7. Comparison between the experimental data for a 7.03×10^{-4} mol dm^{-3} α-alanine solution under hydrothermal conditions in an 'inert' reactor at 155 °C and 20 bar, the calculated data generated from **Model 1**, and the model accuracy and residuals.

them to determine kinetic information, so this data set does not appear in Figs. 11 and 12. Similarly, hydrolysis of dimers was found to have a much lower activation at higher pressures versus the lower saturated vapour pressure. Under both pressure regions, diglycine was found to rapidly cyclize to cyclic diglycine.

The close similarity of α-alanine and glycine (which differ only by one methyl group) and between α-alanine and β-alanine (structural isomers) make it worthwhile to briefly compare these systems. Data on the ionization and speciation of glycine with temperature (Gillespie et al., 1995; Wang et al., 1996; Clarke et al., 2005) exists to a comparable degree as for α-alanine, and provides us with a reasonable assumption that glycine will similarly be present almost entirely as the zwitterion $Hgly^{-+}$ in dilute aqueous solution conditions up to at least 250 °C. The comparisons in Figs. 11 and 12 support the idea that α-alanine, β-alanine and glycine exhibit similar behavior.

Qualitatively speaking, glycine has been the focus of numerous hydrothermal stability studies, particularly in the context of the thermal reactions of food such as the Maillard type reactions. Diglycine and cyclic diglycine (2,5-diketopiperazine) have long been observed to polymerize and became a focus of early amino acid hydrothermal studies (Meggy, 1953; Meggy, 1956; Vallentyne, 1964). Vallentyne (1964) also noted that glycine produced various products including polymers, in contrast to alanine which in his study had only been observed to decarboxylate. More recently, Kohara et al. (1997) proposed polymerization of glycine at elevated temperatures to best explain their observations, and Clarke and Tremaine (1999) found glycine to be less stable than alanine and to form an insoluble precipitate, presumably the result of uncontrolled polymerization. Imai et al. (1999a) and Alargov et al. (2001) were able to form diglycine, triglycine and cyclic diglycine (2,5-diketopiperazine) from aqueous glycine, using a flow reactor at temperatures up to 350 °C which mimicked aspects of a hydrothermal system. Both Qian et al. (1993) and Snider and Wolfenden (2000) observed glycine to be more stable than its polymers in terms of breakdown and/or polymerization. Shiota and Nakashima (2002, 2005) observed the polymerization of glycine that had been produced secondarily from the decomposition of threonine. Faisal et al.

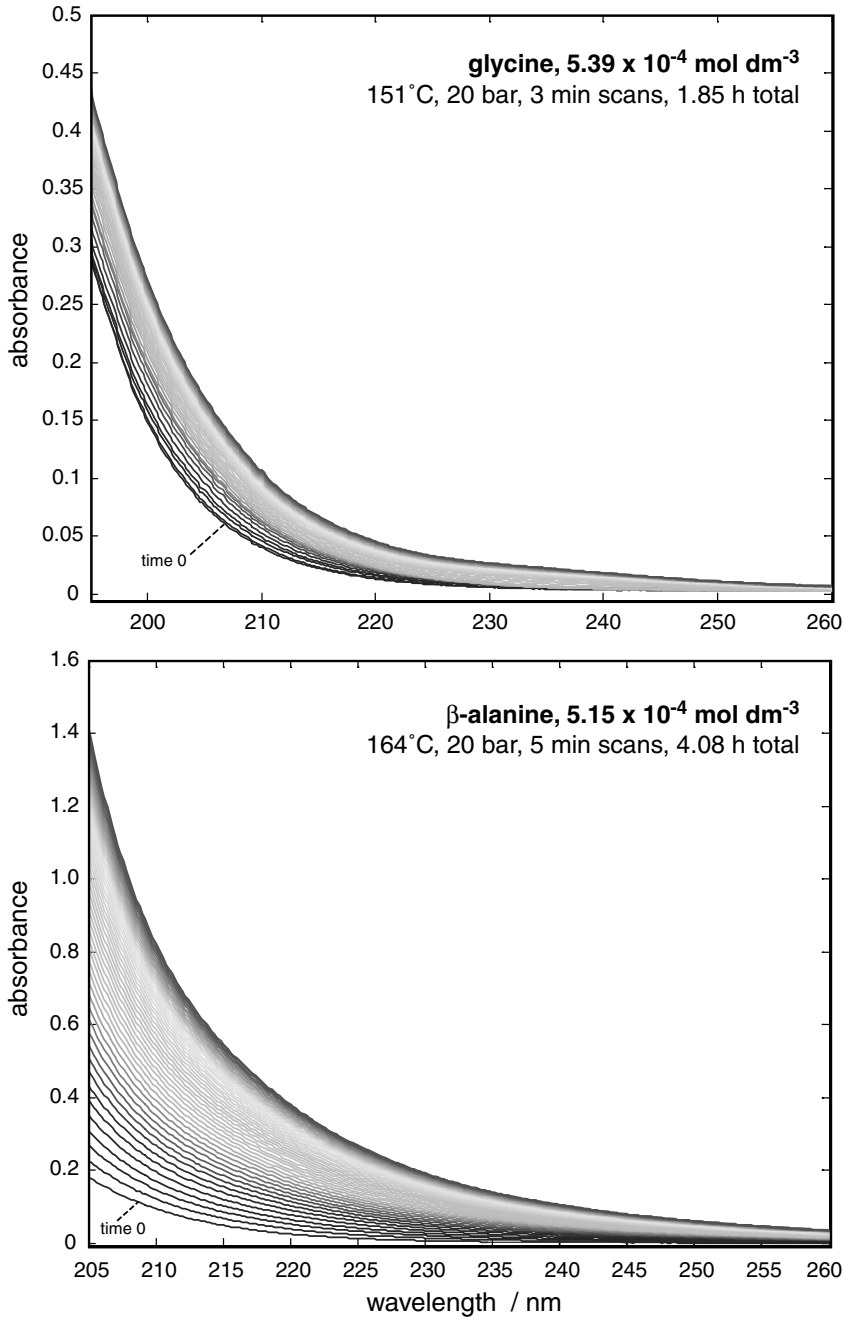

Fig. 8. Examples of UV absorption data sets collected in situ of the thermal evolution of glycine at 151 °C (top) and β-alanine at 164 °C (bottom) aqueous solutions in an 'inert' reactor. Note the greatly expanded absorption scale of β-alanine relative to α-alanine and glycine.

(2005) found clear evidence for the dimerization and cyclization of both glycine and alanine in a simulated hydrothermal vent reactor at 250 °C, and were able to directly confirm the presence of these products in solution, but were unfortunately not able to obtain rate constants due to the complexity of their system. Other observations of polymerization of glycine, using 'simulated hydrothermal vent' type reactors, include Alargov et al. (2002), Goto et al. (2005), Imai et al. (1999b), Islam et al. (2003), Mitsuzawa and Yukawa (2004), Ogata et al. (2000), and Yokoyama et al. (2003).

Although many studies have observed the polymerization of glycine, few have been quantitative with respect to glycine oligomerization and rate constants. No previous measurements of the dimerization of glycine were available. However, the rate constants derived here for glycine are similar to those for α-alanine, which is logical given the similarity of the two amino acids. Regarding the cyclization of diglycine, only the data of Radzicka and Wolfenden (1996) were available, and the data point reproduced here was quoted by the authors as "$>10^{-3}$" because they also had trouble accurately measuring the rate of cyclization. They

Table 3
Rate constants and kinetic information derived from **Model 1** for glycine and β-alanine

Temp (°C)	No. of scans used	Factors	Model	Rate constant k_1 (mol^{-1} dm^3 s^{-1})[a]	Rate constant k_2 (s^{-1})[a]	Instrumental error	Standard deviation of model[b]
glycine							
151.2 ± 0.4	38	3	1	$1.79 \times 10^{-1} \pm 0.03 \times 10^{-1}$	$6.54 \times 10^{-4} \pm 0.05 \times 10^{-4}$	2.0×10^{-4}	4.2×10^{-4}
151.2	38	3	1	$9.8 \times 10^{-2} \pm 0.3 \times 10^{-2}$	$3.38 \times 10^{-4} \pm 0.05 \times 10^{-4}$	2.4×10^{-4}	4.4×10^{-4}
β-alanine							
163.8 ± 0.4	50	3	1	$1.11 \times 10^{-1} \pm 0.03 \times 10^{-1}$	$2.70 \times 10^{-4} \pm 0.04 \times 10^{-4}$	2.0×10^{-4}	4.7×10^{-4}

[a] Error shown is derived from an estimated experimental error margin (5%). In all cases the 3σ confidence limit of the model convergence was very narrow, so the experimental error is taken to be more accurate.
[b] Estimated from the sum of squares of the residuals divided by the number of scans.

alternatively provide an equilibrium constant for the reaction, which at 150 °C was found to be $K = 0.4$. The rate constants presented here for cyclization are in good agreement with their estimated value. Cronin et al. (1971) also present cyclization and hydrolysis data on diglycine and glycylalanine data but it should be noted that these were acquired at slightly lower temperature (95 °C) and in the presence of 0.04 M Zn(II), a catalyst. For β-alanine, no published values of any kind were available for comparison. However, the values of the dimerization and cyclization

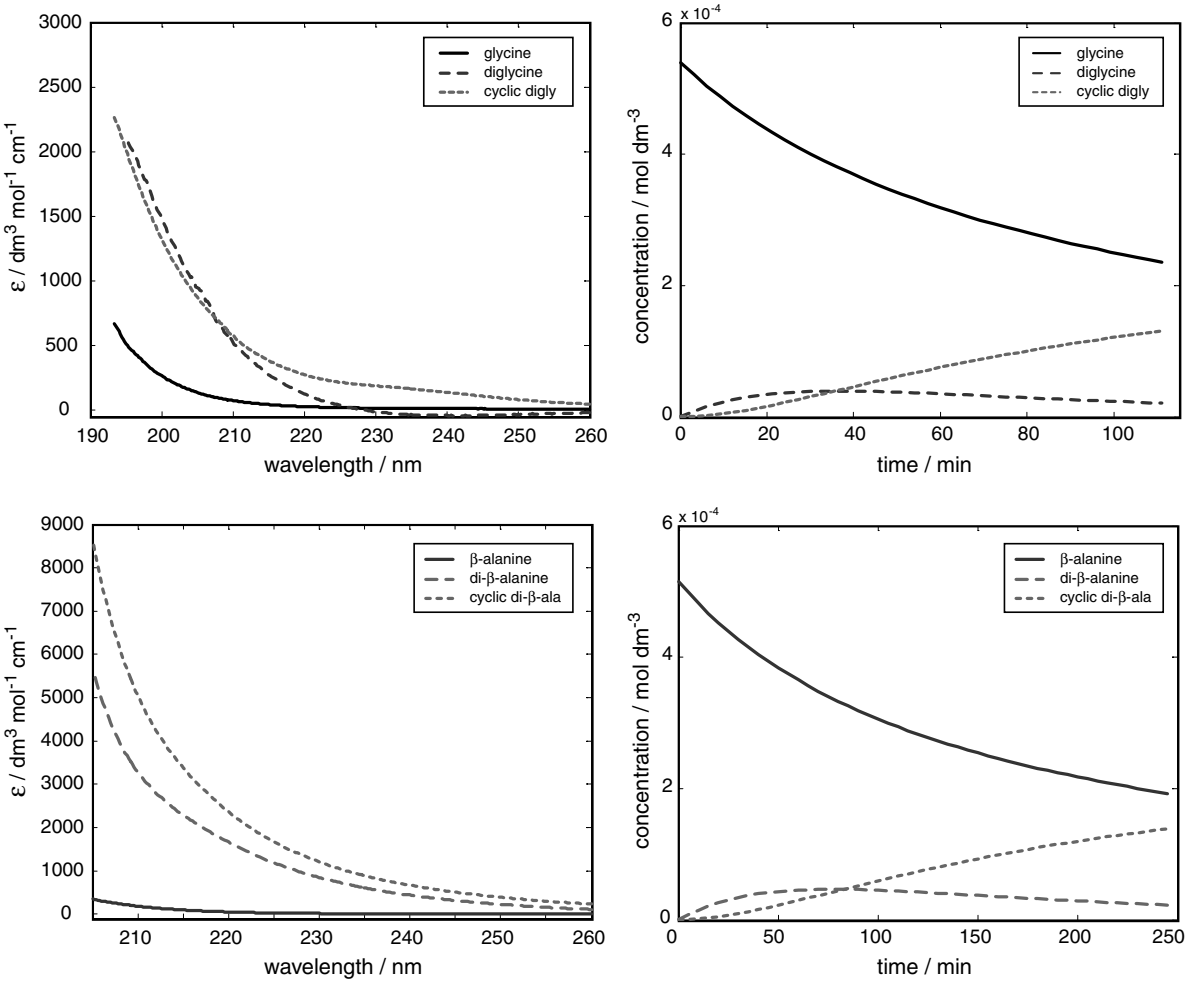

Fig. 9. Calculated molar absorptivities (left) and calculated concentration profiles versus time (right). Aqueous glycine solution (top), 5.39×10^{-4} mol dm^{-3}, at 151 °C and 20 bar; aqueous β-alanine solution (bottom), 5.15×10^{-4} mol dm^{-3}, at 164 °C and 20 bar. Note that the similarities of diglycine and cyclic diglycine under these conditions leads to an increased error in the calculated spectra as the model becomes ill-defined.

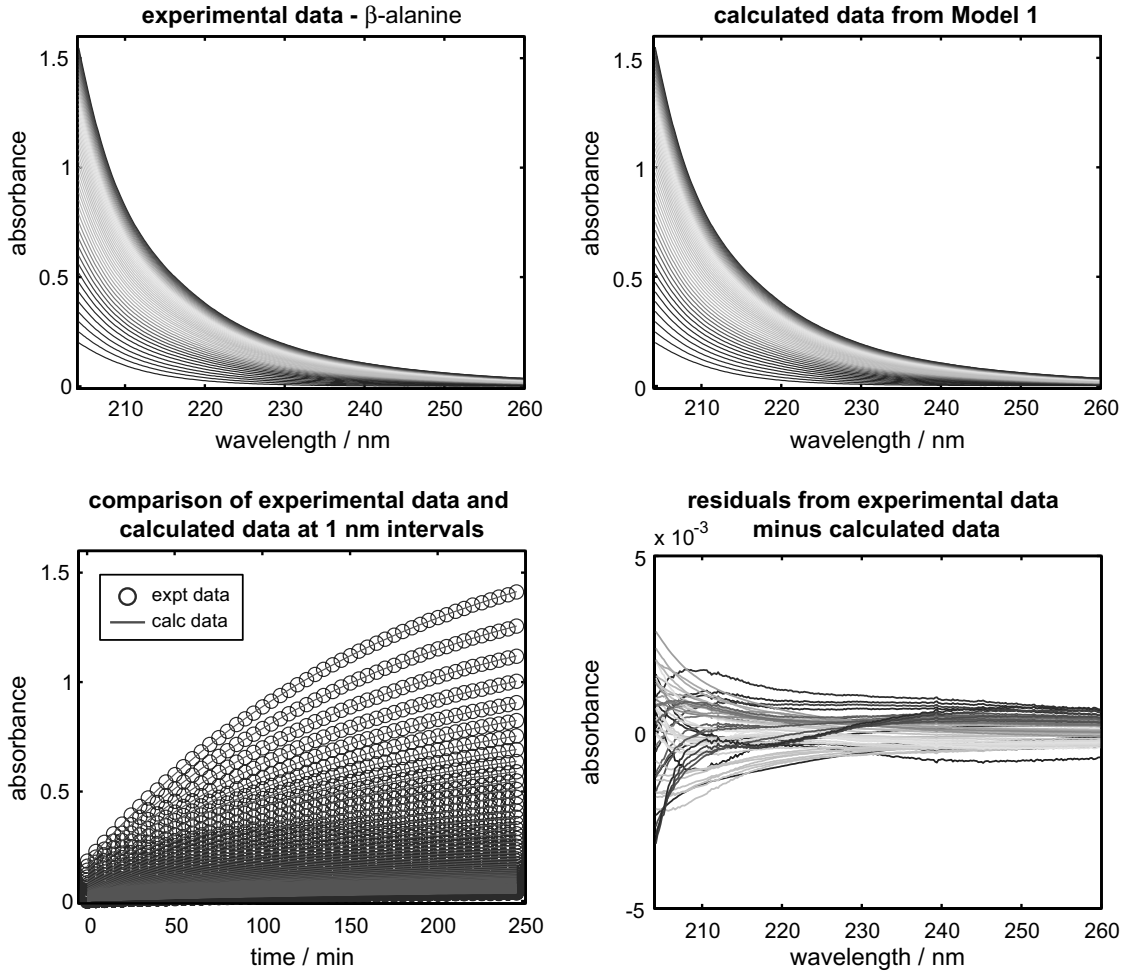

Fig. 10. Comparison between the experimental data for a 5.15×10^{-4} mol dm^{-3} β-alanine solution under hydrothermal conditions in an 'inert' reactor at 164 °C and 20 bar, the calculated data generated from **Model 1**, and the model accuracy and residuals.

rate constants presented here are in a similar range to those for glycine and α-alanine, as expected, since β-alanine (although somewhat different in structure) is an isomer of α-alanine.

5. CONCLUSIONS

This study provides evidence that under certain types of hydrothermal conditions, α-alanine, glycine and β-alanine can preferentially undergo dimerization and cyclization reaction pathways. For α-alanine, the previous work of Radzicka and Wolfenden (1996), Kawamura and Yukioka (2001) and Faisal et al. (2005) similarly point to this conclusion, although the majority of previous studies have observed or assumed decarboxylation as the primary pathway. In the case of glycine there has been long-standing evidence of polymerization (e.g. Meggy, 1953; Meggy, 1956; and Vallentyne, 1964), which has been further supported by recent studies, some of them quantitative (Radzicka and Wolfenden, 1996; Bujdák and Rode, 1997; Clarke and Tremaine, 1999; Imai et al., 1999a; Imai et al., 1999b; Ogata et al., 2000; Alargov et al., 2001; Alargov et al., 2002; Tsukahara et al., 2002; Islam et al., 2003; Yokoyama et al., 2003; Mitsuzawa and Yukawa, 2004; Faisal et al., 2005; Goto et al., 2005; Kawamura et al., 2005; Shiota and Nakashima, 2005).

These differences are principally attributable to variability in experimental conditions. The nature of the surfaces exposed to the analyte solutions surely plays a role (Cox and Seward, 2007), although polymerization has also been observed in stainless steel reactors which were set up as flow-through or cycling systems (e.g. Kawamura and Yukioka, 2001; Faisal et al., 2005; Kawamura et al., 2005). Clearly, factors such as reactor surfaces, temperature, residence time, and matrix components can all play an important role in determining the primary reaction pathways taken by a given system. It is also apparent that more than one combination of factors can lead to polymerization pathways being favored. The collective data available for these systems indicate that polymerization can be a competitive or preferred pathway for small amino acids under a variety of possible conditions. This has important implications for the formation of peptides and

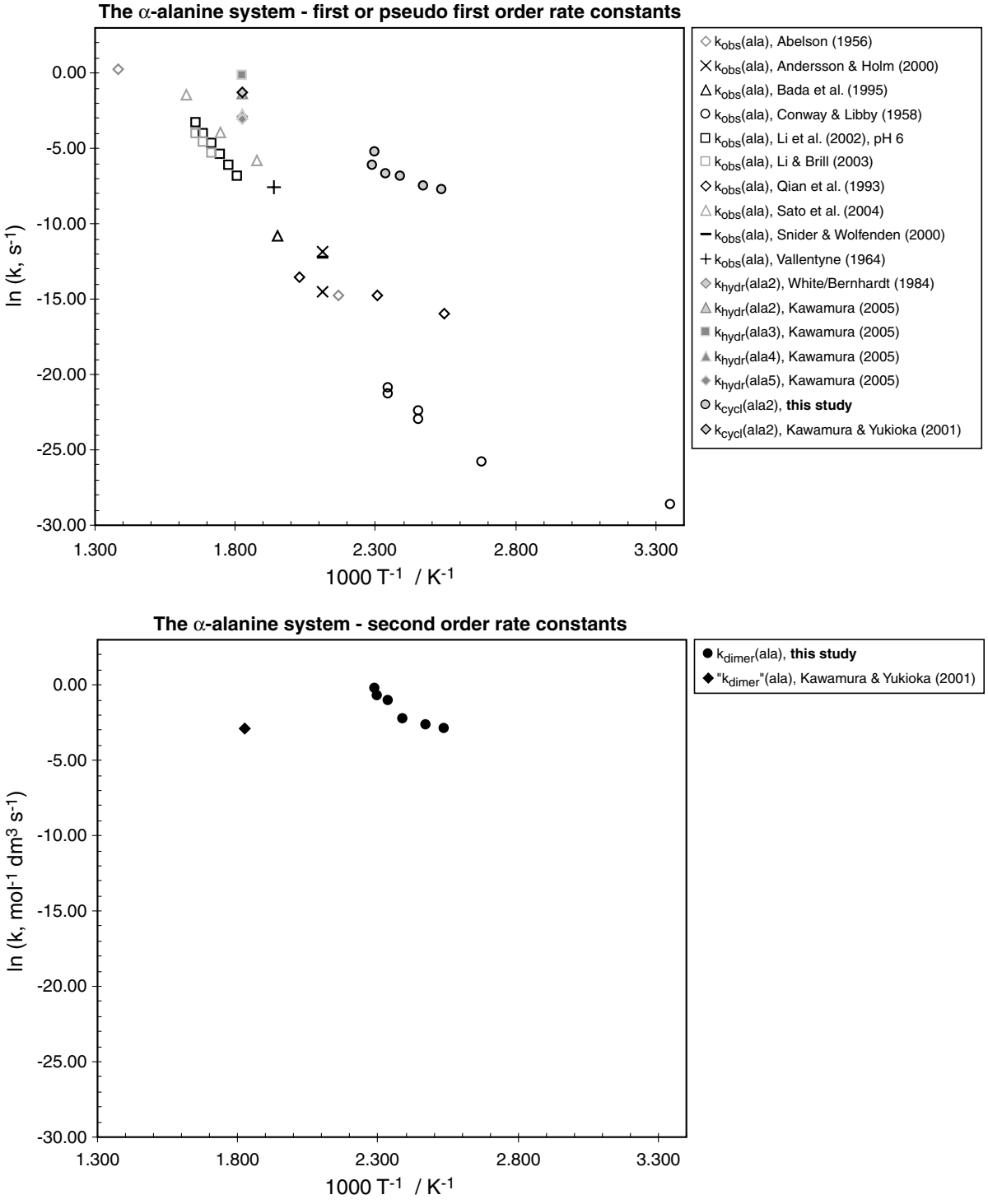

Fig. 11. Comparison of the rate constants derived in this study with previously published rate constants for the hydrothermal stability of the components of the α-alanine system. Type of rate constant is represented by k_{obs} (observed), k_{hydr} (hydrolysis), k_{dimer} (dimerization), and k_{cycl} (cyclization).

other larger molecules under the extreme conditions of seafloor hydrothermal systems. Cyclization to diketopiperazines appears to inhibit further oligomerization to larger peptides, but on the other hand provides a protective effect for small amino acids under high-temperature conditions and acts to stabilize them. It follows that even small amino acids are potentially more stable to breakdown than previously understood, and that polymerization may play an important role under a range of hydrothermal conditions.

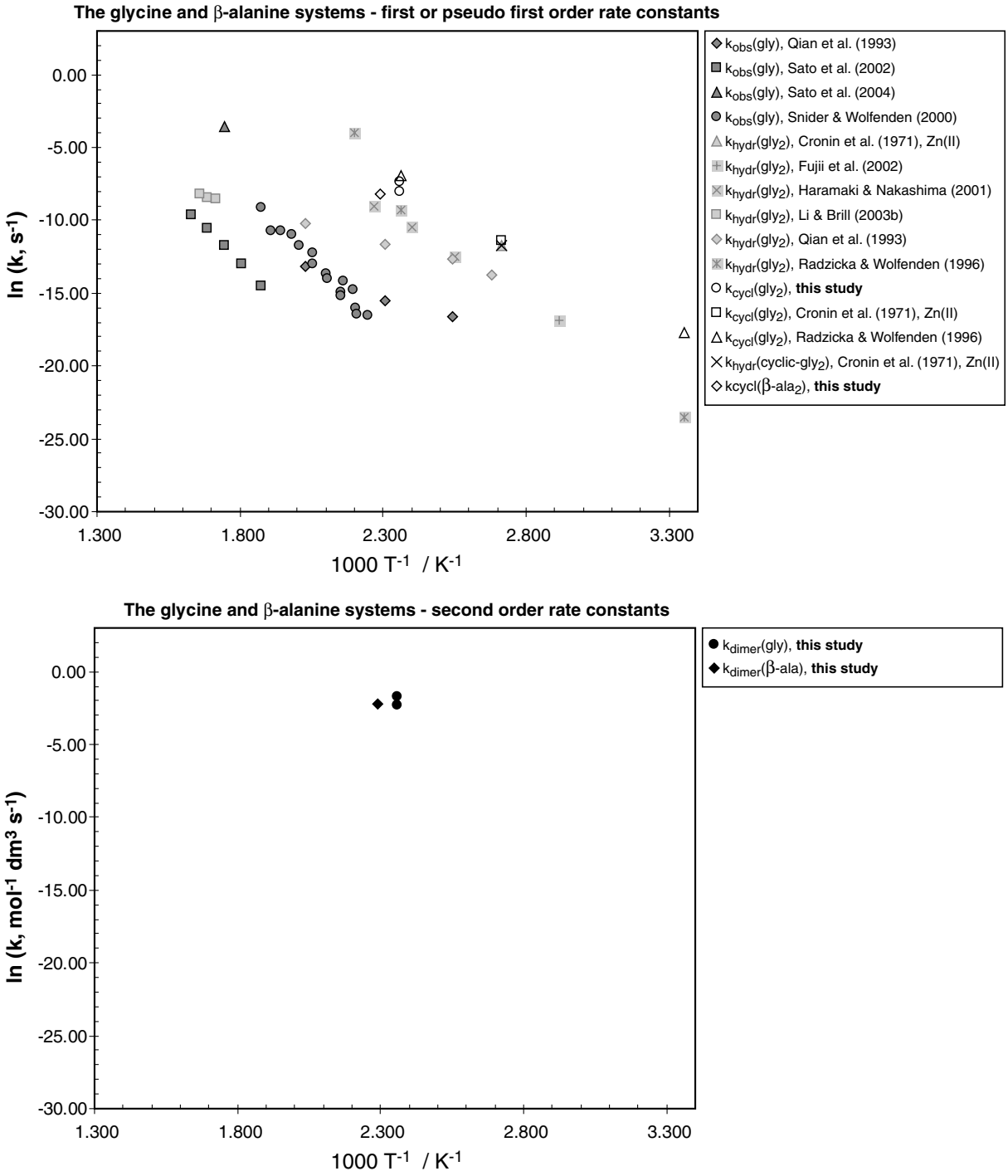

Fig. 12. Comparison of the rate constants derived in this study with previously published rate constants for the hydrothermal stability of the components of the glycine and β-alanine systems. Type of rate constant is represented by k_{obs} (observed), k_{hydr} (hydrolysis), k_{dimer} (dimerization), and k_{cycl} (cyclization).

ACKNOWLEDGMENTS

This work was funded by Swiss National Science Foundation grants #2000-053931 and #2000-061159 awarded to TMS. We would like to express our thanks and appreciation to Jean-François Boily for his valuable assistance and for providing the files used to calculate model errors. JSC would also like to thank Florian Schwandner.

REFERENCES

Abelson P. H. (1956) Amino acids formed in primitive atmospheres. *Science* **124**(3228), 935.

Alargov D., Deguchi S., Tsujii K., and Horikoshi K. (2001) Oligomerization of glycine and synthesis of amino acids in super- and subcritical water; chemical evolution to the origin of life in hydrothermal system. In *Geochemistry and the Origin of*

Life, vol. 2 (eds. S. Nakashima, S. Maruyama, A. Brack and B. Windley). Universal Academy Press, pp. 39–50.

Alargov D. K., Deguchi S., Tsujii K., and Horikoshi K. (2002) Reaction behaviors of glycine under super- and subcritical water conditions. *Orig. Life Evol. Biosph.* **32**(1), 1–12.

Andersson E., and Holm N. (2000) The stability of some selected amino acids under attempted redox constrained hydrothermal conditions. *Orig. Life Evol. Biosph.* **30**(1), 9–23.

Bada J. L., Miller S. L., and Zhao M. (1995) The stability of amino acids at submarine hydrothermal vent temperatures. *Orig. Life Evol. Biosph.* **25**, 111–118.

Bell J., and Palmer D. (1994) Experimental studies of organic acid decomposition. In *Organic Acids in Geological Processes* (eds. E. Pittman and M. Lewan). Springer-Verlag, pp. 226–269.

Bell J. L. S., Palmer D. A., Barnes H. L., and Drummond S. E. (1994) Thermal decomposition of acetate. III. Catalysis by mineral surfaces. *Geochim. Cosmochim. Acta* **58**(19), 4155–4177.

Bernhardt G., Lüdemann H.-D., Jaenicke R., König H., and Stetter K. O. (1984) Biomolecules are unstable under ''black smoker'' conditions. *Naturwissenschaften* **71**, 583–586.

Bujdák J., and Rode B. M. (1997) Glycine oligomerization on silica and alumina. *React. Kinet. Catal. Lett.* **62**(2), 281–286.

Capasso S., Vergara A., and Mazzarella L. (1998) Mechanism of 2,5-dioxopiperazine formation. *J. Am. Chem. Soc.* **120**, 1990–1995.

Christensen J., Oscarson J., and Izatt R. (1968) Thermodynamics of proton ionization in dilute aqueous solution. 10. Delta G degrees (pK) delta H degrees and delta S degrees values for proton ionization from several monosubstituted carboxylic acids at 10, 25 and 40 degrees Celsius. *J. Am. Chem. Soc.* **90**(22), 5949–5953.

Clarke R. G., and Tremaine P. R. (1999) Amino acids under hydrothermal conditions: Apparent molar volumes of aqueous α-alanine, β-alanine, and proline at temperatures from 298 to 523 K and pressures up to 20.0 MPa. *J. Phys. Chem. B* **103**(24), 5131–5144.

Clarke R. G. F., Collins C. M., Roberts J. C., Trevani L. N., Bartholomew R. J., and Tremaine P. R. (2005) Ionization constants of aqueous amino acids at temperatures up to 250 °C using hydrothermal pH indicators and UV–visible spectroscopy: Glycine, α-alanine, and proline. *Geochim. Cosmochim. Acta* **69**(12), 3029–3043.

Conway D., and Libby W. F. (1958) The measurement of very slow reaction rates: decarboxylation of alanine. *J. Am. Chem. Soc.* **80**(5), 1077–1084.

Corliss J. B., Dymond J., Gordon L. I., Edmond J. M., Herzen R. P. V., Ballard R. D., Green K., Williams D., Bainbridge A., Crane K., and Van Andel T. H. (1979) Submarine thermal springs on the Galapagos Rift. *Science* **203**(4385), 1073–1083.

Cox J. S., and Seward T. M. (2007) The hydrothermal reaction kinetics of aspartic acid. *Geochim. Cosmochim. Acta* **71**(4), 797–820.

Cronin J. R., Long D. A., and Truscott T. G. (1971) Peptide kinetics. 12. Effect of zinc(II) on the reaction of some glycine-containing dipeptides and substituted diketopiperazines at pH 5.6 and 368.2 K. *Trans. Faraday Soc.* **67**(7), 2096–2100.

Faisal M., Sato N., Quitain A. T., Daimon H., and Fujie K. (2005) Hydrolysis and cyclodehydration of dipeptide under hydrothermal conditions. *Ind. Eng. Chem. Res.* **44**(15), 5472–5477.

Fujii Y., Kiss T., Gajda T., Tan X. S., Sato T., Nakano Y., Hayashi Y., and Yashiro M. (2002) Copper(II)-*cis*,*cis*-1,3,5-triaminocyclohexane complex-promoted hydrolysis of dipeptides: kinetic, speciation and structural studies. *J. Biol. Inorg. Chem.* **7**(7–8), 843–851.

Gillespie S. E., Oscarson J. L., Izatt R. M., Wang P., Renuncio J. A. R., and Pando C. (1995) Thermodynamic quantities for the protonation of amino acid amino groups from 323.15 to 398.15 K. *J. Solut. Chem.* **24**(12), 1219–1247.

Goto T., Futamura Y., Yamaguchi Y., and Yamamoto K. (2005) Condensation reactions of amino acids under hydrothermal conditions with adiabatic expansion cooling. *J. Chem. Eng. Jpn.* **38**(4), 295–299.

Haramaki T., and Nakashima S. (2001) Thermal decomposition of glycylglycine (Gly-Gly) as studied by by ATR-IR spectroscopy and HPLC (unpublished). Cited in: Nakashima S., and Shiota D. (2001) Organic-inorganic interactions and the origin and evolution of life. In Geochemistry and the Origin of Life, vol. 2 (eds. S. Nakashima, S. Maruyama, A. Brack and B. Windley), Universal Academy Press, pp. 135–178.

Horiuchi T., Takano Y., Ishibashi J., Marumo K., and Kobayashi K. (2004) Amino acids in water samples from deep sea hydrothermal vents at Suiyo Seamount, Izu-Bonin Arc, Pacific Ocean. *Org. Geochem.* **35**(10), 1121–1128.

Imai E.-I., Honda H., Hatori K., and Matsuno K. (1999a) Autocatalytic synthesis of oligoglycine in a simulated submarine hydrothermal system. *Orig. Life Evol. Biosph.* **29**(3), 249–259.

Imai E.-I., Honda H., Hatori K., Brack A., and Matsuno K. (1999b) Elongation of oligopeptides in a simulated submarine hydrothermal system. *Science* **283**(5403), 831–833.

Islam M. N., Kaneko T., and Kobayashi K. (2003) Reaction of amino acids in a supercritical water-flow reactor simulating submarine hydrothermal systems. *Bull. Chem. Soc. Jpn.* **76**(6), 1171–1178.

Kawamura K., and Yukioka M. (2001) Kinetics of the racemization of amino acids at 225–275 degrees C using a real-time monitoring method of hydrothermal reactions. *Thermochim. Acta* **375**(1–2), 9–16.

Kawamura K., Nishi T., and Sakiyama T. (2005) Consecutive elongation of alanine oligopeptides at the second time range under hydrothermal conditions using a microflow reactor system. *J. Am. Chem. Soc.* **127**(2), 522–523.

Kohara M., Gamo T., Yanagawa H., and Kobayashi K. (1997) Stability of amino acids in simulated hydrothermal vent environments. *Chem. Lett.* **10**, 1053.

Li J., Wang X. G., Klein M. T., and Brill T. B. (2002) Spectroscopy of hydrothermal reactions. 19. pH and salt dependence of decarboxylation of α-alanine at 280–330 degrees C in an FT-IR spectroscopy flow reactor. *Int. J. Chem. Kinet.* **34**(4), 271–277.

Li J., and Brill T. B. (2003a) Spectroscopy of hydrothermal reactions. 26: Kinetics of decarboxylation of aliphatic amino acids and comparison with the rates of racemization. *Int. J. Chem. Kinet.* **35**(11), 602–610.

Li J., and Brill T. B. (2003b) Spectroscopy of hydrothermal reactions. 27. Simultaneous determination of hydrolysis rate constants of glycylglycine to glycine and glycylglycine–diketopiperazine equilibrium constants at 310–330 C and 275 bar. *J. Phys. Chem. A* **107**(41), 8575–8577.

Lindsay W. (1980) Estimation of concentration quotients for ionic equilibria in high temperature water: the model substance approach. In Proceedings of the 41st International Water Conference, pp. 284–294.

Malinowski E. R. (1991) *Factor Analysis in Chemistry*. John Wiley & Sons Inc.

Mathworks, Inc. (2000) Matlab R12 / R13 computer software.

Meggy A. B. (1953) Glycine peptides. I. The polymerization of 2,5-piperazinedione at 180 °C. *J. Chem. Soc.*, 851–855.

Meggy A. B. (1956) Glycine peptides. II. The heat and entropy of formation of the peptide bond in polyglycine. *J. Chem. Soc.*, 1444–1454.

Miller S. L. (1953) A production of amino acids under possible primitive earth conditions. *Science* **117**, 528–529.

Miller S. L. (1955) Production of some organic compounds under possible primitive earth conditions. *J. Am. Chem. Soc.* **77**(9), 2351–2361.

Miller S. L., and Urey H. C. (1959) Organic compound synthesis on the primitive earth. *Science* **130**(3370), 245–251.

Mitsuzawa S., and Yukawa T. (2004) A reaction network for triglycine synthesis under hydrothermal conditions. *Bull. Chem. Soc. Jpn.* **77**(5), 965–973.

Nims L. F., and Smith P. K. (1933) The ionization of DL-alanine from twenty to forty-five degrees. *J. Biol. Chem.* **101**, 401.

Ogata Y., Imai E. I., Honda H., Hatori K., and Matsuno K. (2000) Hydrothermal circulation of seawater through hot vents and contribution of interface chemistry to prebiotic synthesis. *Orig. Life Evol. Biosph.* **30**(6), 527–537.

Permyakov E. A., Permyakov S. E., and Medvedkin V. N. (2002) Kinetics and mechanism of the peptide synthesis in solution. *Russ. J. Bioorg. Chem.* **28**(1), 9–13.

Qian Y., Engel M. H., Macko S. A., Carpenter S., and Deming J. W. (1993) Kinetics of peptide hydrolysis and amino acid decomposition at high temperature. *Geochim. Cosmochim. Acta* **57**, 3281–3293.

Radzicka A., and Wolfenden R. (1996) Rates of uncatalyzed peptide bond hydrolysis in neutral solution and the transition state affinities of proteases. *J. Am. Chem. Soc.* **118**(26), 6105–6109.

Sato N., Daimon H., and Fujie K. (2002) Decomposition of glycine in high temperature and high pressure water. *Kagaku Kogaku Ronbunshu* **28**(1), 113–117.

Sato N., Quitain A. T., Kang K., Daimon H., and Fujie K. (2004) Reaction kinetics of amino acid decomposition in high-temperature and high-pressure water. *Ind. Eng. Chem. Res.* **43**(13), 3217–3222.

Shiota D., and Nakashima, S. (2002) Polymerization and decomposition reactions upon heating of an amino acid (threonine) simulating the chemical evolution of life. In *Proceedings of the Japan Earth and Planetary Science Joint Meeting*, Tokyo, Japan, B006–017.

Shiota D., and Nakashima S. (2005) Threonine transformation under hydrothermal conditions. *Chem. Lett.* **34**(2), 158–159.

Smith P., Taylor A., and Smith E. (1937) Thermodynamic properties of solutions of amino acids and related substances. III. The ionization of aliphatic amino acids in aqueous solution from one to fifty degrees. *J. Biol. Chem.* **122**, 109.

Snider M. J., and Wolfenden R. (2000) The rate of spontaneous decarboxylation of amino acids. *J. Am. Chem. Soc.* **122**(46), 11507–11508.

Tsukahara H., Imai E. I., Honda H., Hatori K., and Matsuno K. (2002) Prebiotic oligomerization on or inside lipid vesicles in hydrothermal environments. *Orig. Life Evol. Biosph.* **32**(1), 13–21.

Vallentyne J. R. (1964) Biogeochemistry of organic matter-II. Thermal reaction kinetics and transformation products of amino compounds. *Geochim. Cosmochim. Acta* **28**, 157–188.

Wang P. M., Oscarson J., Gillespie S., Izatt R., and Cao H. (1996) Thermodynamics of protonation of amino acid carboxylate groups from 50 to 125 degrees C. *J. Solut. Chem.* **25**(3), 243–266.

Yokoyama S., Koyama A., Nemoto A., Honda H., Imai E., Hatori K., and Matsuno K. (2003) Amplification of diverse catalytic properties of evolving molecules in a simulated hydrothermal environment. *Orig Life Evol Biosph.* **33**(6), 589–595.

Associate editor: Jeffrey Seewald